

# REGULARIZED FINGERPRINTING IN DETECTION AND ATTRIBUTION OF CLIMATE CHANGE WITH WEIGHT MATRIX OPTIMIZING THE EFFICIENCY IN SCALING FACTOR ESTIMATION

BY YAN LI<sup>1,a</sup>, KUN CHEN<sup>1,b</sup>, JUN YAN<sup>1,c</sup> AND XUEBIN ZHANG<sup>2,d</sup>

<sup>1</sup>*Department of Statistics, University of Connecticut, <sup>a</sup>yan.4.li@uconn.edu, <sup>b</sup>kun.chen@uconn.edu, <sup>c</sup>jun.yan@uconn.edu*

<sup>2</sup>*Division of Climate Research, Environmental and Climate Change Canada, <sup>d</sup>xuebin.zhang@canada.ca*

Detection and attribution analyses play a central role in establishing the causal effect of human activities on global warming. The most commonly used method in such analyses, optimal fingerprinting, is a multiple regression where each covariate has a measurement error whose covariance matrix is the same as that of the regression error up to a known scale. Inferences about the regression coefficients are critical not only for making statements about detection and attribution but also for quantifying the uncertainty in important outcomes derived from detection and attribution analyses. When there are no errors-in-variables (EIV), the optimal weight matrix in estimating the regression coefficients is the precision matrix of the regression error. This matrix, however, is never known and has to be estimated from climate model simulations with regularization. The consequence is that the optimal fingerprinting method is not optimal, as believed in practice. We construct a weight matrix by inverting a nonlinear shrinkage estimate of the error covariance matrix that minimizes loss functions directly targeting the uncertainty of the resulting regression coefficient estimator. The resulting estimator of the regression coefficients is asymptotically optimal as the sample size of the climate model simulations and the matrix dimension go to infinity together with a limiting ratio. When EIVs are present, the estimator of the regression coefficients, based on the proposed weight matrix, is asymptotically more efficient than that based on the inverse of the existing linear shrinkage estimator of the error covariance matrix. The performance of the method is confirmed in finite sample simulation studies mimicking realistic situations in terms of the length of the confidence intervals and empirical coverage rates for the regression coefficients. In an application to detection and attribution analyses of the mean temperature at different spatial scales, the method yielded shorter confidence intervals which are important for such analyses in practice.

**1. Introduction.** Detection and attribution analyses of climate change are critical components in establishing a causal relationship from the human emission of greenhouse gases to the warming of planet Earth (e.g., Bindoff et al. (2013)). In climate science, detection is the process of demonstrating that a climate variable has changed in some defined statistical sense without providing a reason for that change; attribution is the process of evaluating the relative contributions of multiple causal factors to a change or event with an assignment of statistical confidence (e.g., Hegerl and Zwiers (2011)). Casual factors usually refer to external forcings which may be anthropogenic (e.g., greenhouse gases, aerosols, ozone precursors, land use) and/or natural (e.g., volcanic eruptions, solar cycle modulations). By comparing simulated results of climate models with observed climate variables, a detection and attribution analysis evaluates the consistency of observed changes with the expected response, also known as fingerprint, of the climate system under each external forcing.

Optimal fingerprinting is the most widely used method for detection and attribution analyses (e.g., Allen and Stott (2003), Hasselmann (1997), Hegerl et al. (2010)). Fingerprinting

---

Received December 2020; revised March 2022.

*Key words and phrases.* Measurement error, nonlinear shrinkage estimator, total least squares.

is a procedure that regresses the observed climate variable of interest on the fingerprints of external forcings and checks whether the fingerprints are found in and consistent with the observed data. The central target of statistical inferences here is the regression coefficients, also known as scaling factors, which scale the fingerprints of external forcings to best match the observed climate change. Historically, the method was “optimal” in the context of generalized least squares (GLS), when the precision matrix of the regression error is used as weight, such that the resulting estimator of the scaling factors have the smallest variances. It was later recognized that the fingerprint covariates are not observed but estimated from climate model simulations. This leads to an errors-in-variables (EIV) issue which has been approached by the total least squares (TLS) (Allen and Stott (2003)) with both the response and the covariates “prewhitened” by the covariance matrix of the error. The covariance matrix represents the internal climate variation. In practice, it is unknown and has to be estimated from climate model simulations (Allen and Tett (1999), Ribes, Planton and Terray (2013)) which is generally handled preliminarily and independently from the regression inference (e.g., Hannart, Ribes and Naveau (2014)).

Estimating the error covariance matrix in fingerprinting is challenging because the number of available runs from controlled climate model simulations is usually small relative to the dimension of the covariance matrix. The sample covariance matrix is not invertible when the sample size of control runs is less than its dimension. Earlier methods project data onto the leading empirical orthogonal functions (EOF) of the internal climate variability represented by the empirical covariance matrix of the control runs (Hegerl et al. (1996), Allen and Tett (1999)). More recently, the regularized optimal fingerprinting (ROF) method avoids the projection step by a regularized covariance matrix estimation (Ribes, Azaïs and Planton (2009)) based on the linear shrinkage covariance matrix estimator (Ledoit and Wolf (2004)). In the simulation study considered by Ribes, Planton and Terray (2013), the ROF method provides a more robust and accurate implementation of optimal fingerprinting than the EOF projection method, one reason being that the performance of EOF projection can be extremely sensitive to the choice of number of EOFs.

In a Bayesian framework, Katzfuss, Hammerling and Smith (2017) treats the truncation number of EOFs as a parameter which facilitates averaging over different number of truncations for more robust inference. Uncertainties from various sources, such as the error covariance matrix estimation and EIV, can be naturally accounted for. Nonetheless, the Bayesian method is computational intensive, especially for bigger maximum number of truncations; and its performance can be sensitive to the priors. An alternative formulation is given by Hannart (2016) where the closed-form joint likelihood of both the observational data and the control runs is obtained by integrating out the unknown covariance matrix. The integrated method is equivalent to a Bayesian framework with an informative, conjugate prior distribution on the covariance matrix. It allows for shrinkage toward targets from prior information other than the identity matrix, such as one with a spatiotemporal structure used in the numerical studies of Hannart (2016). In real world applications, however, the prior structure on the covariance matrix may not be valid.

The uncertainty in estimating the error covariance matrix has important implications in optimal fingerprinting. The optimality in inferences about the scaling factor in optimal fingerprinting was historically based on the assumption that the error covariance matrix is known. The properties of the scaling factor estimator obtained by substituting the error covariance matrix with an estimate have not been thoroughly investigated in the literature. For example, it is not until recently that the confidence intervals for the scaling factors constructed from asymptotic normal approximation (Fuller (1980), Gleser (1981)) or bootstrap (Pešta (2013)) were reported to be overly narrow when the matrix is only known up to a scale (DelSole et al. (2019)) or completely unknown (Li et al. (2021)). A natural, fundamental question is:

when the error covariance matrix is estimated, are the confidence intervals constructed using the optimal approach under the assumption of known error covariance matrix still optimal? Since optimality under unknown error covariance matrix is practically infeasible, to be precise, we term fingerprinting for optimal fingerprinting and regularized fingerprinting (RF) for ROF in the sequel.

Our work was motivated by a detection and attribution analysis of changes in mean temperature during 1951–2010 at different spatial scales. We develop a new method to construct the weight matrix in RF by minimizing directly the uncertainty of the resulting scaling factor estimators. The weight matrix is the inverse of a nonlinear shrinkage estimator of the error covariance matrix inspired by Ledoit and Wolf (2017a). We first extend the validity of their nonlinear shrinkage estimator to the context of RF via GLS regression with no EIV. We show that the proposed method is asymptotically optimal, as the sample size of climate model simulations and the matrix dimension go to infinity together with a fixed ratio. When there is EIV, as is the case in practice, we show that the proposed weight is more efficient than the existing weight in RF (Ribes, Planton and Terray (2013)) in terms of the asymptotic variance of the scaling factor estimator when RF is conducted with generalized TLS (GTLS). This is why we refer to the current practice by RF instead of ROF. Based on findings of a comparison study under various realistic settings, we give practical recommendations for assumptions about the structure of the error covariance matrix under which the sample covariance is estimated before any shrinkage in RF. In analyzing the motivating application, our method yielded shorter confidence intervals than the competing methods, which have important practical implications, as uncertainty quantification is crucial in detection and attribution analyses. An implementation of our methods is publicly available in an R package `dacc` (Li, Chen and Yan (2020)) for detection and attribution of climate change.

The rest of this article is organized as follows. After a review of RF in Section 2, we develop the proposed weight matrix and the theoretical results to support the asymptotic performance of proposed method in Section 3. A large scale numerical study assessing the performance of the proposed method is reported in Section 4. In Section 5 we apply the proposed method to detection and attribution analysis of changes in mean temperatures on global and regional scales. A discussion concludes in Section 6. The technical proofs of the theoretical results are relegated to the Supplementary Materials (Li et al. (2023)).

**2. Regularized fingerprinting.** Fingerprinting takes the form of a linear regression with EIV,

$$(1) \quad Y = \sum_{i=1}^p X_i \beta_i + \epsilon,$$

$$(2) \quad \tilde{X}_i = X_i + v_i, \quad i = 1, \dots, p,$$

where  $Y$  is a  $N \times 1$  vector of the observed climate variable of interest,  $X_i$  is the true but unobserved  $N \times 1$  fingerprint vector of the  $i$ th external forcing with scaling factor  $\beta_i$ ,  $\epsilon$  is a  $N \times 1$  vector of normally distributed regression error with mean zero and covariance matrix  $\Sigma$ ,  $\tilde{X}_i$  is an estimate of  $X_i$  based on  $n_i$  climate model simulations under the  $i$ th external forcing, and  $v_i$  is a normally distributed measurement error vector with mean zero and covariance matrix  $\Sigma/n_i$ , and  $v_i$ 's are mutually independent and independent of  $\epsilon$ ,  $i = 1, \dots, p$ . The covariance matrices of  $v_i$ 's and  $\epsilon$  only differ in scales under the assumptions that the only source of uncertainty in climate model estimate of fingerprints is the internal climate variability and that the climate models reflect the real climate variation. No intercept is present in the regression because the response and the covariates are centered by the same reference level. The primary target of inference is the scaling factors  $\beta = (\beta_1, \dots, \beta_p)^\top$ .

The “optimal” in optimal fingerprinting originated from earlier practices under two assumptions: 1) the error covariance matrix  $\Sigma$  is known, and 2)  $X_i$ 's are observed. The GLS estimator of  $\beta$  with weight matrix  $W$  is

$$\hat{\beta}(W) = (X^\top W X)^{-1} X^\top W Y,$$

where  $X = (X_1, \dots, X_p)$ . The covariance matrix of the estimator  $\hat{\beta}(W)$  is

$$(3) \quad \mathbb{V}(\hat{\beta}(W)) = (X^\top W X)^{-1} X^\top W \Sigma W X (X^\top W X)^{-1}$$

The optimal weight matrix is  $W = \Sigma^{-1}$ , in which case,  $\hat{\beta}(\Sigma^{-1})$  is the best linear unbiased estimator of  $\beta$  with covariance matrix  $(X^\top \Sigma^{-1} X)^{-1}$ . Since  $\Sigma$  is unknown, a feasible version of GLS uses  $W = \hat{\Sigma}^{-1}$ , where  $\hat{\Sigma}$  is an estimator of  $\Sigma$  obtained separately from controlled runs of climate model simulations.

Later on, it was recognized that, instead of  $X_i$ 's, only their estimates  $\tilde{X}_i$ 's are observed and that using  $\tilde{X}_i$ 's in place of  $X_i$ 's leads to bias in estimating  $\beta$  (Allen and Stott (2003)). If  $\Sigma$  is given, the same structure (up to a scale  $1/n_i$ ) of the covariance matrices of  $v_i$ 's and  $\epsilon$  allows precise prewhitening of both  $Y$  and  $\tilde{X}_i$ 's. Then, the TLS can be applied to the prewhitened variables. Inferences about  $\beta$  can be based on the asymptotic normal distribution of the TLS estimator of  $\beta$  (Gleser (1981), Allen and Stott (2003)) or nonparametric bootstrap (Peřta (2013)), as recently studied by DelSole et al. (2019). Similar to the GLS setting, a feasible version of the GTLS procedure relies on an estimator of  $\Sigma$ .

The current practice of fingerprinting consists of two separate steps. First, estimate  $\Sigma$  from controlled runs of climate model simulations under the assumption that the climate models capture the internal variability of the real climate system. Second, use this estimated matrix to prewhiten both the outcome and covariates in the regression model (1)–(2), and obtain the GTLS estimator of  $\beta$  on the prewhitened data. Nonetheless, estimation of  $\Sigma$  in the first step is not an easy task. The dimension of  $\Sigma$  is  $N \times N$ , with  $N(N + 1)/2$  parameters if no structure is imposed, which is too large for the sample size  $n$  of available climate model simulations (usually in a few hundreds at most). The sample covariance matrix, based on the  $n$  runs, is a start, but it is of too much variation; when  $N > n$ , it is not even invertible. The linear shrinkage method of Ledoit and Wolf (2004) regularizes the sample covariance matrix  $\hat{\Sigma}_n$  to in the form of  $\lambda \hat{\Sigma}_n + \rho I$ , where  $\lambda$  and  $\rho$  are scalar tuning parameters and  $I$  is the identity matrix. This class of shrinkage estimators has the effect of shrinking the set of sample eigenvalues by reducing its dispersion around the mean, pushing up the smaller ones and pulling down the larger ones. This estimator has been used in the current RF practice (Ribes, Azaïs and Planton (2009), Ribes, Planton and Terray (2013)).

Substituting  $\Sigma$  with an estimator introduces an additional uncertainty. The impact of this uncertainty on the properties of resulting ROF estimator has not been investigated when the whole structure of  $\Sigma$  is unknown (Li et al. (2021)). The optimality of the optimal fingerprinting in its original sense is unlikely to still hold. Now that the properties of the resulting estimator of  $\beta$  depends on an estimated weight matrix, can we choose this weight matrix estimator to minimize the variance of the estimator of  $\beta$ ? The recently proposed nonlinear shrinkage estimator (Ledoit and Wolf (2017a, 2018)) has high potential to outperform the linear shrinkage estimators.

**3. Weight matrix construction.** We consider constructing the weight matrix by inverting a nonlinear shrinkage estimator of  $\Sigma$  (Ledoit and Wolf (2017b)) in the fingerprinting context. New theoretical results are developed to justify the adaptation of this nonlinear shrinkage estimator of  $\Sigma$  to minimize the uncertainty of the resulting estimator  $\hat{\beta}$  of  $\beta$ . Assume that there are  $n$  replicates from climate model simulations (usually preindustrial control runs) that

are independent of  $Y$  and  $\tilde{X}_i$ 's. Let  $Z_1, Z_2, \dots, Z_n \in \mathbb{R}^N$  be the centered replicates so that the sample covariance matrix is computed as  $\hat{\Sigma}_n = n^{-1} \sum_{i=1}^n Z_i Z_i^\top$ . Our strategy is to revisit the GLS setting with no EIV first and then apply the result of the GTLS setting to the case under EIV, the same order as the historical development.

3.1. *GLS.* Since the target of inference is  $\beta$ , we propose to minimize the ‘‘total variation’’ of the covariance matrix  $\mathbb{V}(\hat{\beta})$  of the estimated scale factors  $\hat{\beta}(W)$  in (3) with respect to  $W = \hat{\Sigma}^{-1}$ . Two loss functions are considered that measure the variation of  $\hat{\beta}$ , namely, the summation of the variances of  $\hat{\beta}$  (trace of  $\mathbb{V}(\hat{\beta})$ ) and the general variance of  $\hat{\beta}$  (determinant of  $\mathbb{V}(\hat{\beta})$ ), denoted, respectively, as  $L_1(\hat{\Sigma}, \Sigma, X)$  and  $L_2(\hat{\Sigma}, \Sigma, X)$ . In particular, we have

$$L_1(\hat{\Sigma}, \Sigma, X) = \text{Tr}((X^\top \hat{\Sigma}^{-1} X)^{-1} X^\top \hat{\Sigma}^{-1} \Sigma \hat{\Sigma}^{-1} X (X^\top \hat{\Sigma}^{-1} X)^{-1}),$$

$$L_2(\hat{\Sigma}, \Sigma, X) = \left(\frac{\text{Tr}(X^\top X)}{pN}\right)^p \det\left(\frac{X^\top \hat{\Sigma}^{-1} \Sigma \hat{\Sigma}^{-1} X}{N}\right) \det^{-2}\left(\frac{X^\top \hat{\Sigma}^{-1} X}{N}\right),$$

where the first loss function directly targets on the trace of  $\mathbb{V}(\hat{\beta}(W))$  and the second loss function is proportional to the determinant of  $\mathbb{V}(\hat{\beta}(W))$  (up to a constant scale  $\{\text{Tr}(X^\top X)/p\}^p$ ).

The theoretical development is built on minimizing the limiting forms of the loss functions as  $n \rightarrow \infty$  and  $N \rightarrow \infty$ . The special case of  $p = 1$  has been approached by Ledoit and Wolf (2017b). We extend their result to multiple linear regressions with  $p > 1$ .

LEMMA 1. *The loss functions  $L_1(\hat{\Sigma}, \Sigma, X)$  and  $L_2(\hat{\Sigma}, \Sigma, X)$  remain unchanged after orthogonalization of design matrix  $X$  via the singular value decomposition.*

The proof of Lemma 1 is Appendix A, Supplementary Material (Li et al. (2023)).

Lemma 1 implies that, without loss of generality, we only need to consider orthogonal designs in the regression model (1). In other words, we may assume that the columns of the design matrix  $X$  are such that  $X_i^\top X_j = 0$  for any  $i \neq j$ .

Consider the minimum variance loss function

$$(4) \quad L_{\text{mv}}(\hat{\Sigma}, \Sigma) = \frac{\text{Tr}(\hat{\Sigma}^{-1} \Sigma \hat{\Sigma}^{-1})/N}{(\text{Tr}(\hat{\Sigma}^{-1})/N)^2}$$

derived in Engle, Ledoit and Wolf (2019). We have the following result.

THEOREM 1. *As dimension  $N \rightarrow \infty$  and sample size  $n \rightarrow \infty$  with  $N/n \rightarrow c$  for a constant  $c$ , minimizing  $\lim_{n, N \rightarrow \infty} L_1(\hat{\Sigma}, \Sigma, X)$  or  $\lim_{n, N \rightarrow \infty} L_2(\hat{\Sigma}, \Sigma, X)$ , is equivalent to minimizing  $\lim_{n, N \rightarrow \infty} L_{\text{mv}}(\hat{\Sigma}, \Sigma)$ .*

The proof for Theorem 1 is presented in Appendix B, Supplementary Material (Li et al. (2023)).

Let  $\hat{\Sigma}_n = \Gamma_n D_n \Gamma_n^\top$  be the spectral decomposition of the sample covariance matrix  $\hat{\Sigma}_n$ , where  $D_n = \text{diag}(\lambda_1, \dots, \lambda_N)$  is the diagonal matrix of the eigenvalues and  $\Gamma_n$  contains the corresponding eigenvectors. Consider the rotation invariant class of the estimators  $\hat{\Sigma} = \Gamma_n \tilde{D}_n \Gamma_n^\top$ , where  $\tilde{D}_n = \text{diag}(\delta(\lambda_1), \dots, \delta(\lambda_N))$  for a smooth function  $\delta(\cdot)$ . Then, under some regularity assumptions on the data generation mechanism (Ledoit and Wolf (2017a), Assumptions 1–4), we can get the asymptotically optimal estimator  $\hat{\Sigma}$  which minimizes the limiting form of proposed two loss functions as  $n \rightarrow \infty$  and  $N \rightarrow \infty$ .

Let  $F_N$  be the empirical cumulative distribution function of sample eigenvalues. Silverstein (1995) showed that the limiting form  $F = \lim_{N, n \rightarrow \infty} F_N$  exists under the same assumptions. The oracle optimal nonlinear shrinkage estimator, minimizing the limiting form of proposed

loss function under general asymptotics, depends only on the derivative  $f = F'$  of  $F$  and its Hilbert transform  $\mathcal{H}_f$ , and the limiting ratio  $c$  of  $N/n$  (Ledoit and Wolf (2017a)) with the shrinkage form of the eigenvalues given by

$$(5) \quad \delta_{\text{oracle}}(\lambda_i) = \frac{\lambda_i}{[\pi c \lambda_i f(\lambda_i)]^2 + [1 - c - \pi c \lambda_i \mathcal{H}_f(\lambda_i)]^2}.$$

A feasible nonlinear shrinkage estimator (*bona fide* counterpart of the oracle estimator) can be based on a kernel estimator of  $f$  which is proposed and shown by Ledoit and Wolf (2017a) to perform as well as the oracle estimator asymptotically. Let  $c_n = N/n$  which is an estimator for the limiting concentration ratio  $c$ . The feasible nonlinear shrinkage  $\delta(\lambda_i)$ ,  $i = 1, \dots, N$ , of the sample eigenvalues is defined as following results for both cases of  $c_n \leq 1$  and  $c_n > 1$ .

Case 1. If  $c_n \leq 1$ , that is, the sample covariance matrix is nonsingular, then

$$\delta(\lambda_i) = \frac{\lambda_i}{[\pi \frac{N}{n} \lambda_i \tilde{f}(\lambda_i)]^2 + [1 - \frac{N}{n} - \pi \frac{N}{n} \lambda_i \mathcal{H}_{\tilde{f}}(\lambda_i)]^2},$$

where  $\tilde{f}(\cdot)$  is a kernel estimator of the limiting sample spectral density  $f$  and  $\mathcal{H}_{\tilde{f}}$  is the Hilbert transform of  $\tilde{f}$ . Various authors adopt different conventions to define the Hilbert transform. We follow Ledoit and Wolf (2017a) and apply the same semicircle kernel function and Hilbert transform because of the consistency of the resulting feasible estimator. Specifically, we have

$$\begin{aligned} \tilde{f}(\lambda_i) &= \frac{1}{N} \sum_{j=1}^N \frac{\sqrt{[4\lambda_j^2 h_n^2 - (\lambda_i - \lambda_j)^2]^+}}{2\pi \lambda_j^2 h_n^2}, \\ \mathcal{H}_{\tilde{f}}(\lambda_i) &= \frac{1}{N} \sum_{j=1}^N \frac{\text{sgn}(\lambda_i - \lambda_j) \sqrt{[(\lambda_i - \lambda_j)^2 - 4\lambda_j^2 h_n^2]^+} - \lambda_i + \lambda_j}{2\pi \lambda_j^2 h_n^2}, \end{aligned}$$

where  $h_n = n^{-\gamma}$  is the bandwidth of the semicircle kernel with tuning parameter  $\gamma$  and  $a^+ = \max(0, a)$ . For details on the Hilbert transform and the mathematical formulation of Hilbert transform for commonly used kernel functions, see Bateman (1954).

Case 2. In optimal fingerprinting applications the case of  $c_n > 1$  is more relevant because the number  $n$  of controlled runs that can be used to estimate the internal climate variation is often limited, much less than the dimension  $N$  of the problem. If  $c_n > 1$ , we have  $N - n$  null eigenvalues. Assume that  $(\lambda_1, \dots, \lambda_{N-n}) = 0$ . In this case we only consider the empirical cumulative distribution function  $\underline{F}_N$  of the nonzero  $n$  eigenvalues. From Silverstein (1995), there existing a limiting function  $\underline{F}$  such that  $\lim_{N,n \rightarrow \infty} \underline{F}_N = \underline{F}$ , and it admits a continuous derivative  $\underline{f}$ . The oracle estimator in equation (5) can be written as

$$\delta_{\text{oracle}}(\lambda_i) = \frac{\lambda_i}{\pi^2 \lambda_i^2 [\underline{f}(\lambda_i)^2 + \mathcal{H}_{\underline{f}}(\lambda_i)^2]}.$$

Then, the kernel approach can be adapted in this case. Let  $\tilde{\underline{f}}$  and  $\mathcal{H}_{\tilde{\underline{f}}}$  be, respectively, the kernel estimator for  $\underline{f}$  and its Hilbert transform  $\mathcal{H}_{\underline{f}}$ . The feasible shrinkage estimator is

$$\begin{aligned} \delta(0) &= \frac{1}{\pi \frac{N-n}{n} \mathcal{H}_{\tilde{\underline{f}}}(0)}, \quad i = 1, \dots, N - n, \\ \delta(\lambda_i) &= \frac{\lambda_i}{\pi^2 \lambda_i^2 [\tilde{\underline{f}}(\lambda_i)^2 + \mathcal{H}_{\tilde{\underline{f}}}(\lambda_i)^2]}, \quad i = N - n + 1, \dots, N, \end{aligned}$$

where

$$\begin{aligned} \mathcal{H}_{\underline{f}}(0) &= \frac{1 - \sqrt{1 - 4h_n^2}}{2\pi n h_n^2} \sum_{j=N-n+1}^N \frac{1}{\lambda_j}, \\ \underline{f}(\lambda_i) &= \frac{1}{n} \sum_{j=N-n+1}^N \frac{\sqrt{[4\lambda_j^2 h_n^2 - (\lambda_i - \lambda_j)^2]^+}}{2\pi \lambda_j^2 h_n^2}, \\ \mathcal{H}_{\underline{f}}(\lambda_i) &= \frac{1}{n} \sum_{j=N-n+1}^N \frac{\text{sgn}(\lambda_i - \lambda_j) \sqrt{[(\lambda_i - \lambda_j)^2 - 4\lambda_j^2 h_n^2]^+} - \lambda_i + \lambda_j}{2\pi \lambda_j^2 h_n^2}, \end{aligned}$$

and  $h_n = n^{-\gamma}$  is the bandwidth with tuning parameter  $\gamma$ .

In both cases the pool-adjacent-violators-algorithm (PAVA) in isotonic regression can be used to ensure the shrunken eigenvalues to be in ascending order. The bandwidth parameter  $\gamma$  can be selected via cross validation on the estimated standard deviation of the scaling factors or other information criteria. The feasible optimal nonlinear shrinkage estimator is the resulting  $\hat{\Sigma}_{MV} = \Gamma_n \tilde{D}_n \Gamma_n^\top$ , where MV stands for minimum variance.

3.2. *GTLS*. For the GTLS setting, which is more realistic with EIV, we propose to prewhiten  $Y$  and  $\tilde{X}_i$ 's by  $\hat{\Sigma}_{MV}$  and then apply the standard TLS procedure (Gleser (1981)) to estimate  $\beta$ . The resulting estimator of the  $\beta$  will be shown to be more efficient than that based on prewhitening with the linear shrinkage estimator  $\hat{\Sigma}_{LS}$  (Ribes, Planton and Terray (2013)).

Consider the GTLS estimator of  $\beta$  obtained from prewhitening with a class of regularized covariance matrix estimator  $\hat{\Sigma}$  from independent control runs. In the general framework of GTLS, the measurement error vectors usually have the same covariance matrix as the model error vector for the ease of theoretical derivations. This assumption can be easily achieved in the OF setting (1)–(2) by multiplying each observed fingerprint vector  $\tilde{X}_i$  by  $\sqrt{n_i}$ . Therefore, without loss of generality, in the following we assume  $n_i = 1$  to simplify the notations.

Let  $\tilde{X} = (\tilde{X}_1, \dots, \tilde{X}_p)$  and  $\beta_0 \in \mathbb{R}^p$  be the true coefficient vector for the fingerprints. The GTLS estimator based on  $\hat{\Sigma}$  is

$$(6) \quad \hat{\beta}(\hat{\Sigma}) = \arg \min_{\beta} \frac{\|\hat{\Sigma}^{-\frac{1}{2}}(Y - \tilde{X}\beta)\|_2^2}{1 + \beta^\top \beta},$$

where  $\|a\|_2$  is the  $\ell_2$  norm of vector  $a$ . The asymptotic properties of  $\hat{\beta}(\hat{\Sigma})$  are established for a class of covariance matrix estimators  $\hat{\Sigma}$ , including both  $\hat{\Sigma}_{MV}$  and  $\hat{\Sigma}_{LS}$ .

ASSUMPTION 1.  $\lim_{N,n \rightarrow \infty} X^\top \hat{\Sigma}^{-1} X / N = \Delta_1$  exists, where  $\Delta_1$  is a nonsingular matrix.

ASSUMPTION 2.  $\lim_{N,n \rightarrow \infty} \text{Tr}(\hat{\Sigma}^{-1} \Sigma) / N$  exists and is a positive constant.

ASSUMPTION 3.  $\lim_{N,n \rightarrow \infty} \text{Tr}\{(\hat{\Sigma}^{-1/2} \Sigma \hat{\Sigma}^{-1/2})^2\} / N = K$  exists with  $K > 0$ .

REMARK 1. Assumption 1 originates from Gleser (1981) which is needed for the consistency of  $\hat{\beta}(\hat{\Sigma})$ . Assumptions 2–3 are from Ledoit and Wolf (2017a, 2018). Assumption 2 states that the average of the variances of the components of the prewhitened error vectors converge to positive constant. For the class of rotation invariant estimators defined in Ledoit and Wolf (2017a, 2017b), which includes both  $\hat{\Sigma}_{MV}$  and  $\hat{\Sigma}_{LS}$ , Assumptions 2 and 3 are satisfied.

LEMMA 2. Under Assumptions 1–3,  $\hat{\beta}(\hat{\Sigma}) \xrightarrow{\mathcal{P}} \beta_0$ , as  $N, n \rightarrow \infty$  with a  $N/n \rightarrow c$  for some  $c > 0$ .

The proof for Lemma 2 is in Appendix C, Supplementary Material (Li et al. (2023)). The asymptotic normality of  $\hat{\beta}(\hat{\Sigma})$  is established with additional assumptions.

ASSUMPTION 4.  $\lim_{N,n \rightarrow \infty} X^\top \hat{\Sigma}^{-1} \Sigma \hat{\Sigma}^{-1} X / N = \Delta_2$  exists for a nonsingular matrix  $\Delta_2$ .

ASSUMPTION 5. The regression error  $\epsilon$  and measurement errors  $v_i$ 's,  $i = 1, \dots, p$ , are mutually independent normally distributed random vectors.

REMARK 2. Assumption 4 originates from Gleser (1981) for the asymptotic normality of the GTLS estimator. Assumption 5 is commonly used in the context of climate change detection and attribution for mean state climate variables.

THEOREM 2. Under Assumptions 1–5, as  $N, n \rightarrow \infty$  with  $N/n \rightarrow c$  for some  $c > 0$ ,

$$(7) \quad \sqrt{N}(\hat{\beta} - \beta_0) \xrightarrow{\mathcal{D}} \mathcal{N}(0, \Xi), \text{ where } \Xi = \Delta_1^{-1} \{ \Delta_2 + K(I_p + \beta_0 \beta_0^\top) \} (1 + \beta_0^\top \beta_0) \Delta_1^{-1}.$$

The proof of Theorem 2 is in Section C.2 of Appendix C, Supplementary Material (Li et al. (2023)).

The higher efficiency of the resulting estimator for  $\beta$  from the proposed weight matrix in comparison with that from the existing weight is summarized by the following result with proof in Section C.3 of Appendix C, Supplementary Material (Li et al. (2023)).

THEOREM 3. Let  $\Xi(\hat{\Sigma})$  be the asymptotic covariance matrix in equation (7) for a rotation invariant estimator  $\hat{\Sigma}$  under Assumptions 1–5. Then,  $\text{Tr}(\Xi(\hat{\Sigma}_{\text{MV}})) \leq \text{Tr}(\Xi(\hat{\Sigma}_{\text{LS}}))$ .

The proofs of Theorem 3 is in Section C.3 of Appendix C, Supplementary Material (Li et al. (2023)).

In our implementation, a five-fold cross validation is used to select the optimal bandwidth parameter  $\gamma \in (0.2, 0.5)$ .

**4. Simulation studies.** The finite sample performance of the proposed method in comparison with the existing practice in RF needs to be assessed to make realistic recommendations for detection and attribution of climate change. We conducted a simulation study similar to the setting of a study in Ribes, Planton and Terray (2013). The observed climate variable of interest is 11 decadal mean temperatures over 25 grid boxes, a vector of dimension  $N = 275$ . Two  $N \times 1$  fingerprints were considered, corresponding to the anthropogenic (ANT) and natural forcings (NAT), denoted by  $X_1$  and  $X_2$ , respectively. They were set to the average of all runs from the CNRM-CM5 model, as in Ribes, Planton and Terray, 2013. To vary the strength of the signals, we also considered halving  $X_1$  and  $X_2$ . That is, there were two levels of signal-to-noise ratio corresponding to the cases of multiplying each  $X_i$ ,  $i \in \{1, 2\}$ , controlled by a scale  $\lambda \in \{1, 0.5\}$ . The case of  $\lambda = 1$  is corresponding to a global study with strong signal strength, while the  $\lambda = 0.5$  matches with regional studies where the signals are weaker. The true scaling factors were  $\beta_1 = \beta_2 = 1$ . The distribution of the error vector  $\epsilon$  was multivariate normal  $\text{MVN}(0, \Sigma)$ . The distribution of the measurement error vector  $v_i$ ,  $i \in \{1, 2\}$ , was  $\text{MVN}(0, \Sigma/n_i)$ , with  $(n_1, n_2) = (35, 46)$ , which are the values in the detection and attribution analysis of annual mean temperature conducted in Section 5. The

observed mean temperature vector  $Y$  and the estimated fingerprints  $(\tilde{X}_1, \tilde{X}_2)$  were generated from Models (1)–(2). The control runs used to estimate  $\Sigma$  were generated from  $MVN(0, \Sigma)$  with sample size  $n \in \{50, 100, 200, 400\}$ .

Two settings of true  $\Sigma$  were considered. In the first setting,  $\Sigma$  was an unstructured matrix  $\Sigma_{UN}$  which was obtained by manipulating the eigenvalues but keeping the eigenvectors of the proposed minimum variance estimate from the same set of climate model simulations as in Ribes, Planton and Terray, 2013. Specifically, we first obtained the eigen decomposition of the minimum variance estimate, and then restricted the eigenvalues to be equal over each of the 25 grid boxes (i.e., only 25 unique values for the  $N = 25 \times 11$  eigenvalues) by taking averages over the decades at each grid box. The pattern of the resulting eigenvalues is similar to the pattern of the eigenvalues of a spatial-temporal covariance matrix with variance stationarity and weak dependence over the time dimension. Finally, the eigenvalues were scaled independently by a uniformly distributed variable on  $[0.5, 1.5]$  which results in a more unstructured covariance matrix setting similar to the simulation settings in Hannart (2016). In the second setting,  $\Sigma$  was set to be  $\Sigma_{ST}$ , a separable spatiotemporal covariance matrix; the diagonals were set to be the sample variances from the climate model simulations without imposing temporal stationarity; the corresponding correlation matrix was set to be the Kronecker product of a spatial correlation matrix and a temporal correlation matrix, both with autoregressive of order 1 and coefficient 0.1.

For each configuration, 1000 replicates were generated. For each replicate, the two GTLS estimators of  $\beta$  in Theorem 3 were obtained. The one based on prewhitening matrix  $\hat{\Sigma}_{LS}$  is denoted as LS. The one based on prewhitening matrix  $\hat{\Sigma}_{MV}$  is denoted as MV. For comparison, we also obtained the estimator from the Bayesian hierarchical model Katzfuss, Hammerling and Smith (2017), denoted by BH with the code from Dr. Dori Hammerling, and the estimator from the integrated likelihood method of Hannart (2016), denoted by IN with our own implementation. In the Bayesian hierarchical method we implemented the model for the number of principal components  $r \in \{1, \dots, 25\}$  and took average over all the choices. In the integrated approach, since the true covariance matrix is unstructured, we considered the noninformative shrinkage target, the identity matrix.

Figure 1 displays the boxplots of the point estimates of the ANT scaling factor  $\beta_1$  from the four methods: LS, MV, BH, and IN. The shrinkage-based estimators LS, MV, and IN appear to recover the true parameter values well on average. The BH estimator tends to underestimate the true coefficients possibly due to the complexity of the true covariance matrix, which echoes the findings in the numerical studies of Katzfuss, Hammerling and Smith (2017), that the estimation of regression coefficients are shrunk toward zero. The variations of all estimators are lower for larger  $n$ , higher  $\lambda$ , and more structured  $\Sigma$  (the case of  $\Sigma_{ST}$ ).

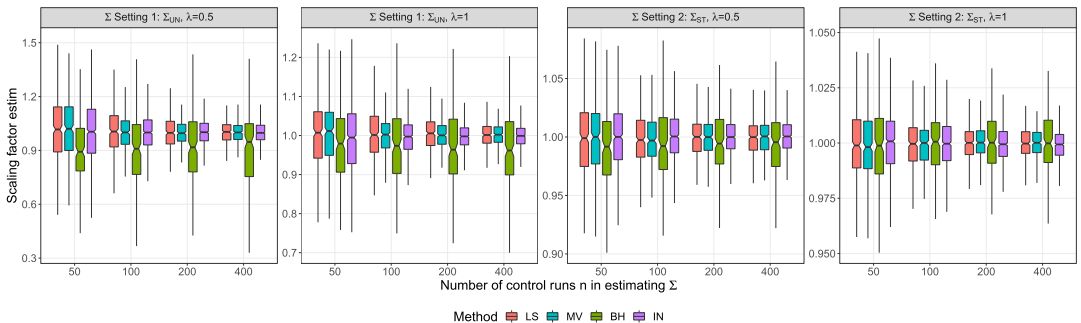


FIG. 1. Boxplots of the estimates of the ‘ANT’ scaling factor obtained from the ROF approach with four estimators, LS, MV, BH, and IN, based on 1000 replicates. The number of ensembles for estimating the ‘ANT’ and ‘NAT’ signals are  $n_1 = 35$  and  $n_2 = 46$ , respectively.

These observations are expected. A larger  $n$  means more accurate estimation of  $\Sigma$ ; a higher  $\lambda$  means stronger signal; a more structured  $\Sigma$  means an easier task to estimate  $\Sigma$ . In general, the Bayesian approach BH has much larger bias and variations than the shrinkage based method LS, MV, and IN. Since we only considered the noninformative target, the IN estimator performs almost identically to the LS estimator, with the LS method having a slightly smaller variations. When  $\Sigma = \Sigma_{\text{UN}}$ , the MV estimates have smaller variations than the LS or IN estimate, since the eigenvalues were less smooth and, hence, favored the nonlinear shrinkage function. When  $\Sigma = \Sigma_{\text{ST}}$ , which is more structured, all the three shrinkage-based methods estimate the true covariance matrix more accurately, and their differences are less obvious. More detailed results are summarized in Web Table 1 and Web Table 2 in the Supplementary Material (Li et al. (2023)), the latter of which had smaller ensembles in estimating the fingerprints with  $(n_1, n_2) = (10, 6)$ . The standard deviations of the MV estimates are over 10% smaller than those of the LS (or IN) estimates for both cases.

Confidence intervals are an important tool for detection and attribution analyses. It would be desirable if the asymptotic variance in Theorem 2 can be used to construct confidence intervals for the scaling factors. Unfortunately, it has been reported that the confidence intervals constructed for the scaling factors, based on  $\hat{\Sigma}_{\text{LS}}$ , have coverage rates lower than, sometimes much lower than, their nominal levels (Hannart (2016), Li et al. (2021)). The under-coverage issue remains for the estimator based on  $\hat{\Sigma}_{\text{MV}}$ . To alleviate the problem, the prevailing practice is to obtain two independent estimators for the unknown covariance matrix by partitioning the available simulations into two independent samples, one used in estimating the scaling factors and the other used in constructing their confidence intervals. Nonetheless, as reported by Li et al. (2021), this approach does not solve the problem, as it was hoped for and performs similarly to the methods based on asymptotic normality, especially under a completely unknown structure of  $\Sigma$ . As a remedy, Li et al. (2021) proposed a calibration procedure which enlarges the confidence intervals based on the asymptotic normality of the estimators by an appropriate scale tuned by a parametric bootstrap to achieve the desired coverage rate. We applied this calibration approach to both the LS and the MV estimators. For the BH estimator, we constructed 95% credible intervals and recorded the corresponding lengths from the posterior distribution. For the IN estimator, because of its similarity to the LS estimator, we used the the same scaling ratios tuned for the LS estimator to enlarge its confidence intervals.

Figure 2 shows the empirical coverage rates of the 95% calibrated confidence intervals for LS, MV, and IN and credible intervals for BH. The BH method has much lower coverage rates than the nominal level with longer intervals than the proposed method in most cases, except for sample size  $n = 50$ . For all three shrinkage-based methods the coverage rates of the confidence intervals before calibration could be as low as 70% (not shown). After calibration, the coverage rates are much closer to the nominal levels. The agreement is better for larger  $n$  and more structured  $\Sigma$ . The calibrated MV confidence intervals are about 10% shorter than the LS intervals and slightly shorter than the IN intervals overall in both  $\Sigma$  settings. The only exception is for the case of  $\Sigma = \Sigma_{\text{UN}}$  and sample size  $n = 50$  where the calibrated confidence intervals still suffer from under-coverage issue. The under-coverage issue is less satisfactorily solved for the IN method which could be improved by finding its own calibration scales. Overall, the proposed MV method outperforms the existing competitors in terms of interval estimation in addition to point estimation.

**5. Fingerprinting mean temperature changes.** We apply the proposed approach to the detection and attribution analyses of annual mean temperature of 1951–2010 at the global (GL), continental, and subcontinental scales. The continental scale regions are Northern Hemisphere (NH), NH midlatitude between 30° and 70° (NHM), Eurasia (EA), and North America (NA) which were studied in (Zhang, Zwiers and Stott (2006)). The subcontinental

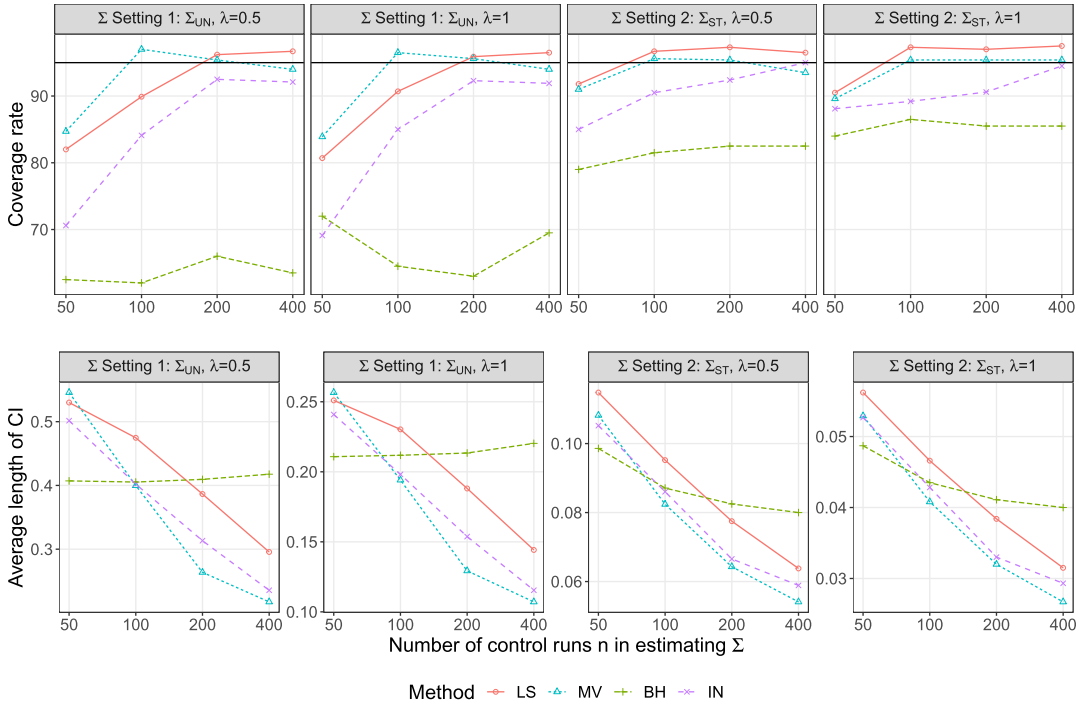


FIG. 2. Estimated coverage rates and lengths of calibrated 95% confidence intervals for the “ANT” scaling factor constructed from four estimators, LS, MV, BH, and IN, based on 1000 replicates. The number of ensembles for estimating the ‘ANT’ and ‘NAT’ signals are  $n_1 = 35$  and  $n_2 = 46$ , respectively.

scale regions are Western North American (WNA), Central North American (CNA), Eastern North American (ENA), southern Canada (SCA), and southern Europe (SEU), where the spatiotemporal correlation structure is more likely to hold.

In each regional analysis we first constructed observation vector  $Y$  from the HadCRUT4 dataset (Morice et al. (2012)). The raw data were monthly anomalies of near-surface air temperature on  $5^\circ \times 5^\circ$  grid boxes. At each grid box, each annual mean temperature was computed from monthly temperatures if at least nine months were available in that year; otherwise, it was considered missing. Then, five-year averages were computed if no more than two annual averages were missing. To reduce the spatial dimension in the analyses, the  $5^\circ \times 5^\circ$  grid boxes were aggregated into larger grid boxes. In particular, the grid-box sizes were  $40^\circ \times 30^\circ$  for GL and NH,  $40^\circ \times 10^\circ$  for NH 30-70,  $10^\circ \times 20^\circ$  for EA, and  $10^\circ \times 5^\circ$  for NA. For the subcontinent regions, no aggregation was done, except for SCA, in which case  $10^\circ \times 10^\circ$  grid boxes were used. Details on the longitude, latitude, and spatiotemporal steps of each regions after processing can be found in Table 1.

Two external forcings, ANT and NAT, were considered. Their fingerprints  $X_1$  and  $X_2$  were not observed, but their estimates  $\tilde{X}_1$  and  $\tilde{X}_2$  were averages over  $n_1 = 35$  and  $n_2 = 46$  runs from CIMP5 climate model simulations. The missing pattern in  $Y$  was used to mask the simulated runs. The same procedure used to aggregate the grid boxes and obtain the five-year averages in preparing  $Y$  was applied to each masked run of each climate model under each forcing. The final estimates  $\tilde{X}_1$  and  $\tilde{X}_2$  at each grid box were averages over all available runs under the ANT and the NAT forcings, respectively, centered by the average of the observed annual temperatures over 1961–1990, the same center used by the HadCRUT4 data to obtain the observed anomalies.

Estimation of  $\Sigma$  was based on  $n = 223$  runs of 60 years constructed from preindustrial control simulations of various length; see Web Table 3 in Appendix E, Supplementary Ma-

TABLE 1

Summaries of the names, coordinate ranges, ideal spatiotemporal dimensions ( $S$  and  $T$ ), and dimension of observation after removing missing values of the five regions analyzed in the study

Acronym	Regions	Longitude (°E)	Latitude (°N)	Grid size ( $1^\circ \times 1^\circ$ )	$S$	$T$	$n$
Global and Continental Regions							
GL	Global	−180/180	−90/90	$40 \times 30$	54	11	572
NH	Northern Hemisphere	−180/180	0/90	$40 \times 30$	27	11	297
NHM	Northern Hemisphere $30^\circ N$ to $70^\circ N$	−180/180	30/70	$40 \times 10$	36	11	396
EA	Eurasia	−10/180	30/70	$10 \times 20$	38	11	418
NA	North America	−130/−50	30/60	$10 \times 5$	48	11	512
Subcontinental Regions							
WNA	Western North America	−130/−105	30/60	$5 \times 5$	30	11	329
CNA	Central North America	−105/−85	30/50	$5 \times 5$	16	11	176
ENA	Eastern North America	−85/−50	15/30	$5 \times 5$	21	11	231
SCA	Southern Canada	−110/−10	50/70	$10 \times 10$	20	11	220
SEU	South Europe	−10/40	35/50	$5 \times 5$	30	11	330

terial (Li et al. (2023)). The long-term linear trend was removed separately from the control simulations at each grid box. As the internal climate variation is assumed to be stationary over time, each control run was first split into nonoverlapping blocks of 60 years, and then each 60-year block was masked by the same missing pattern as the HadCRUT4 data to create up to 12 five-year averages at each grid box. The temporal stationarity of variance at each grid implies equal variance over time steps at each observing grid box which is commonly incorporated in detection and attribution analyses of climate change (e.g., Hannart (2016)). Both LS and MV estimates based on linear and nonlinear shrinkage, respectively, were obtained for comparison. Pooled estimation of the variance at each grid box was considered in each of the shrinkage estimation to enforce the stationary, grid-box specific variance.

Figure 3 summarizes the GTLS estimates of the scaling factors  $\hat{\beta}_1$  and  $\hat{\beta}_2$  for the ANT and NAT forcings, respectively. The estimates from prewhitening weight matrix  $\Sigma_{LS}$  and  $\Sigma_{MV}$  are denoted again as LS and MV, respectively. The 95% confidence intervals were obtained with the calibration approach of Li et al. (2021). The point estimates from LS and MV are similar in all the analysis. The confidence intervals from the MV method are generally shorter than those from the LS method in the analyses both at continental and subcontinental scale. More obvious reduction in the confidence interval lengths is observed at the subcontinental scales, for example, the ANT scaling factor in EA/NA/SCA and the NAT scaling factor in NA/WNA/SCA. This may be explained by that signals at subcontinental scale are weaker and that the error covariance matrix has nonsmooth eigenvalues that form some clustering patterns due to weak temporal dependence, as suggested by the simulation study. Although the detection and attribution conclusions based on the confidence intervals remain the same in most cases, the shortened confidence intervals means reduced uncertainty in the estimate of the attributable warming (Jones, Stott and Christidis (2013)) and other quantities based on detection and attribution analysis, such as future climate projection and transient climate sensitivity (Li et al. (2021)).

**6. Discussion.** Optimal fingerprinting, as the most commonly used method for detection and attribution analyses of climate change, has great impact in climate research. Such analyses are the basis for projecting observationally constrained future climate (e.g., Jones, Stott and Mitchell (2016)) and estimating important properties of the climate system such as climate sensitivity (e.g., Schurer et al. (2018)). The original optimality of optimal fingerprinting,

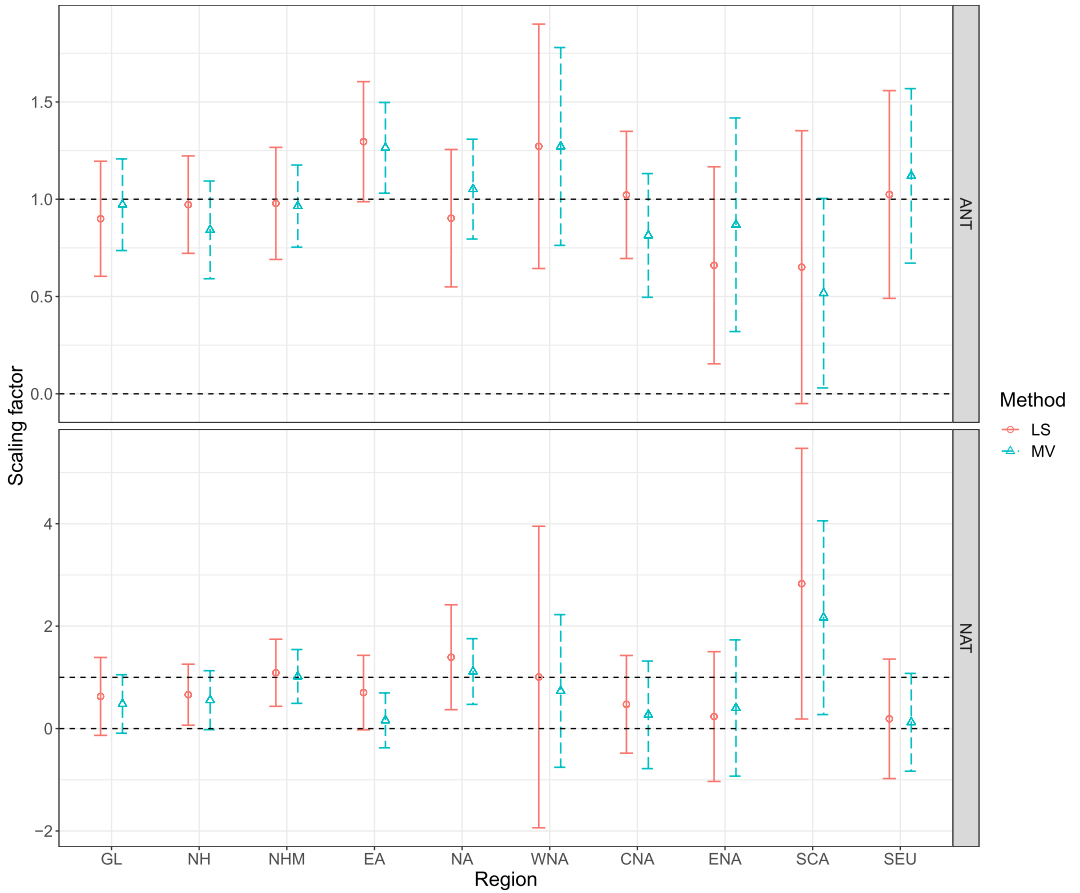


FIG. 3. Estimated signal scaling factors for ANT and NAT required to best match observed 1950–2010 annual mean temperature for different spatial domains, and the corresponding 95% confidence intervals from different methods. For weight matrix construction, “LS” denotes the linear shrinkage approach, and “MV” denotes the minimum variance approach. For confidence interval the calibration method is used.

which minimizes the uncertainty in the resulting scaling factor estimator, is no longer valid under realistic settings where  $\Sigma$  is not known but estimated. Our method constructs a weight matrix by inverting a nonlinear shrinkage estimator of  $\Sigma$  which directly minimizes the variation of the resulting scaling factor estimator. This method is more efficient than the current RF practice (Ribes, Planton and Terray (2013)), as evident from the simulation study. Therefore, the lost optimality in fingerprinting is restored to a good extent for practical purposes, which helps to reduce the uncertainty in important quantities, such as attributable warming and climate sensitivity.

There are open questions that we have not addressed. It is of interest to further investigate how the asymptotic results under  $N, n \rightarrow \infty$  and  $N/n \rightarrow c$  can guide the RF practice. The temporal and spatial resolution that controls  $N$  can be tuned in RF practice, which may lead to different efficiencies in inferences and, hence, different results in detection and attribution. Is there an optimal temporal/spatial resolution to obtain the most reliable result? Goodness-of-fit check is an important element in detection and attribution analyses. The classic approach to check the weighted sum of squared residuals against a chi-squared distribution, under the assumption of known  $\Sigma$  is not valid when  $\Sigma$  has to be estimated. Can a test be designed, possibly based on parametric bootstrap, to take into account of the uncertainty in regularized estimation of  $\Sigma$ ? These questions merit future research.

**Funding.** JY's research was partially supported by NSF Grant DMS-1521730. KC's research was partially supported by NSF Grant IIS-1718798.

## SUPPLEMENTARY MATERIAL

**Appendices and figures/tables referenced in the text** (DOI: [10.1214/22-AOAS1624SUPPA](https://doi.org/10.1214/22-AOAS1624SUPPA); .pdf). A) Sufficiency to Assume Orthogonal Covariates; B) Justification of Method MV in the GLS Case; C) Justification of Method MV in the GTLS Case; D) Detailed Results on Simulation Studies; E) Details of the CMIP5 climate models for the control runs.

**Source code and data** (DOI: [10.1214/22-AOAS1624SUPPB](https://doi.org/10.1214/22-AOAS1624SUPPB); .zip). The data and code used to reproduce the simulation study and data analysis are contained in a zipped file `Rcodesdacc.zip`. R functions used in the analysis are also publicly available in an R package `dacc` (Li, Chen and Yan (2020)) for detection and attribution of climate change.

## REFERENCES

- ALLEN, M. R. and STOTT, P. A. (2003). Estimating signal amplitudes in optimal fingerprinting, Part I: Theory. *Clim. Dyn.* **21** 477–491.
- ALLEN, M. R. and TETT, S. F. B. (1999). Checking for model consistency in optimal fingerprinting. *Clim. Dyn.* **15** 419–434.
- BATEMAN, H. (1954). *Tables of Integral Transforms II*. McGraw-Hill, New York.
- BINDOFF, N. L., STOTT, P. A., ACHUTARAO, K. M., ALLEN, M. R., GILLETT, N., GUTZLER, D., HANSINGO, K., HEGERL, G., HU, Y. et al. (2013). Detection and attribution of climate change: From global to regional. In *Climate Change 2013: The Physical Science Basis. Contribution of Working Group I to the Fifth Assessment Report of the Intergovernmental Panel on Climate Change* (T. F. Stocker, D. Qin, G. K. Plattner, M. Tignor, S. K. Allen, J. Boschung, A. Nauels, Y. Xia, V. Bex et al., eds.) 867–952 10. Cambridge Univ. Press, Cambridge, United Kingdom and New York, NY, USA. <https://doi.org/10.1017/CBO9781107415324.022>
- DELSOLE, T., TRENARY, L., YAN, X. and TIPPETT, M. K. (2019). Confidence intervals in optimal fingerprinting. *Clim. Dyn.* **52** 4111–4126.
- ENGLER, R. F., LEDOIT, O. and WOLF, M. (2019). Large dynamic covariance matrices. *J. Bus. Econom. Statist.* **37** 363–375. [MR3948411 https://doi.org/10.1080/07350015.2017.1345683](https://doi.org/10.1080/07350015.2017.1345683)
- FULLER, W. A. (1980). Properties of some estimators for the errors-in-variables model. *Ann. Statist.* **8** 407–422. [MR0560737](https://doi.org/10.1214/aos/1176345673)
- GLESER, L. J. (1981). Estimation in a multivariate “errors in variables” regression model: Large sample results. *Ann. Statist.* **9** 24–44. [MR0600530](https://doi.org/10.1214/aos/1176345630)
- HANNART, A. (2016). Integrated optimal fingerprinting: Method description and illustration. *J. Climate* **29** 1977–1998.
- HANNART, A., RIBES, A. and NAVEAU, P. (2014). Optimal fingerprinting under multiple sources of uncertainty. *Geophys. Res. Lett.* **41** 1261–1268.
- HASSELMANN, K. (1997). Multi-pattern fingerprint method for detection and attribution of climate change. *Clim. Dyn.* **13** 601–611.
- HEGERL, G. and ZWIERS, F. (2011). Use of models in detection and attribution of climate change. *Wiley Interdiscip. Rev.: Clim. Change* **2** 570–591.
- HEGERL, G. C., VON STORCH, H., HASSELMANN, K., SANTER, B. D., CUBASCH, U. and JONES, P. D. (1996). Detecting greenhouse-gas-induced climate change with an optimal fingerprint method. *J. Climate* **9** 2281–2306.
- HEGERL, G. C., HOEGH-GULDBERG, O., CASASSA, G., HOERLING, M. P., KOVATS, R. S., PARMESAN, C., PIERCE, D. W. and STOTT, P. A. (2010). Good practice guidance paper on detection and attribution related to anthropogenic climate change. In *Meeting Report of the Intergovernmental Panel on Climate Change Expert Meeting on Detection and Attribution of Anthropogenic Climate Change* (T. F. Stocker, C. B. Field, D. Qin, V. Barros, G. K. Plattner, M. Tignor, P. M. Midgley and K. L. Ebi, eds.) IPCC Working Group I Technical Support Unit, Univ. Bern, Bern, Switzerland.
- JONES, G. S., STOTT, P. A. and CHRISTIDIS, N. (2013). Attribution of observed historical near-surface temperature variations to anthropogenic and natural causes using CMIP5 simulations. *J. Geophys. Res., Atmos.* **118** 4001–4024.
- JONES, G. S., STOTT, P. A. and MITCHELL, J. F. B. (2016). Uncertainties in the attribution of greenhouse gas warming and implications for climate prediction. *J. Geophys. Res., Atmos.* **121** 6969–6992.

- KATZFUSS, M., HAMMERLING, D. and SMITH, R. L. (2017). A Bayesian hierarchical model for climate change detection and attribution. *Geophys. Res. Lett.* **44** 5720–5728.
- LEDOIT, O. and WOLF, M. (2004). A well-conditioned estimator for large-dimensional covariance matrices. *J. Multivariate Anal.* **88** 365–411. MR2026339 [https://doi.org/10.1016/S0047-259X\(03\)00096-4](https://doi.org/10.1016/S0047-259X(03)00096-4)
- LEDOIT, O. and WOLF, M. (2017a). Direct nonlinear shrinkage estimation of large-dimensional covariance matrices Working Paper No. 264 Univ. Zurich, Department of Economics.
- LEDOIT, O. and WOLF, M. (2017b). Nonlinear shrinkage of the covariance matrix for portfolio selection: Markowitz meets Goldilocks. *Rev. Financ. Stud.* **30** 4349–4388. <https://doi.org/10.1093/rfs/hhx052>
- LEDOIT, O. and WOLF, M. (2018). Optimal estimation of a large-dimensional covariance matrix under Stein's loss. *Bernoulli* **24** 3791–3832. MR3788189 <https://doi.org/10.3150/17-BEJ979>
- LI, Y., CHEN, K. and YAN, J. (2020). dacc: Detection and Attribution of Climate Change. R package version 0.1-13.
- LI, Y., CHEN, K., YAN, J. and ZHANG, X. (2021). Uncertainty in optimal fingerprinting is underestimated. *Environ. Res. Lett.* **16** 084043.
- LI, Y., CHEN, K., YAN, J. and ZHANG, X. (2023). Supplement to “Regularized fingerprinting in detection and attribution of climate change with weight matrix optimizing the efficiency in scaling factor estimation.” <https://doi.org/10.1214/22-AOAS1624SUPPA>, <https://doi.org/10.1214/22-AOAS1624SUPPB>
- MORICE, C. P., KENNEDY, J. J., RAYNER, N. A. and JONES, P. D. (2012). Quantifying uncertainties in global and regional temperature change using an ensemble of observational estimates: The HadCRUT4 data set. *J. Geophys. Res., Atmos.* **117** D08101.
- PEŠTA, M. (2013). Total least squares and bootstrapping with applications in calibration. *Statistics* **47** 966–991. MR3175728 <https://doi.org/10.1080/02331888.2012.658806>
- RIBES, A., AZAÏS, J.-M. and PLANTON, S. (2009). Adaptation of the optimal fingerprint method for climate change detection using a well-conditioned covariance matrix estimate. *Clim. Dyn.* **33** 707–722.
- RIBES, A., PLANTON, S. and TERRAY, L. (2013). Application of regularised optimal fingerprinting to attribution. Part I: Method, properties and idealised analysis. *Clim. Dyn.* **41** 2817–2836.
- SCHURER, A., HEGERL, G., RIBES, A., POLSON, D., MORICE, C. and TETT, S. (2018). Estimating the transient climate response from observed warming. *J. Climate* **31** 8645–8663.
- SILVERSTEIN, J. W. (1995). Strong convergence of the empirical distribution of eigenvalues of large-dimensional random matrices. *J. Multivariate Anal.* **55** 331–339. MR1370408 <https://doi.org/10.1006/jmva.1995.1083>
- ZHANG, X., ZWIERS, F. and STOTT, P. A. (2006). Multimodel multisignal climate change detection at regional scale. *J. Climate* **19** 4294–4307.